Journal of Civil Engineering
The Institution of Engineers, Bangladesh
Vol. CE 26 No. 2, 1998

HEATING EFFECTS OF PAVEMENT ON URBAN THERMAL ENVIRONMENT

Muhammad Abu Eusuf[1] and Takashi Asaeda[2]

ABSTRACT : Heat fluxes at the air/ground interface together with temperature in the surface and the subsurface of heterogeneous pavements were observed and analysed on summer days. It was found that the surface and subsurface temperatures of various pavement materials were significantly different from each other. Temperature at the porous and nonporous asphalt pavement at the peak hour was more than 52°C, which was 17°C higher than air temperature and that of other porous blocks also reached about 50°C. However temperature of the ceramic pavement was much lower than that of other surfaces and almost as same as that of the grass surface. Results of the computation using a numerical model reveals that the pore size is very important for the transport of water vapor in the pavement.

KEY WORDS: Porous Pavement, Nonporous Pavement, Urban Environment, Heating Effects, Pore Volume, Sealed Surface.

INTRODUCTION

Heating effects of ground surface on the thermal environment is done for purpose of understanding and in some cases controlling the behavior and properties of the macroscopic medium. The concept of what is 'macroscopic' is spontaneous one and it usually means a sample of the medium on which observation are performed in the field (Dullier 1991). Heating effects of ground surface are an important factor in the surface energy balance. It represents the energy flux available for the transport of sensible and latent heat to the atmosphere above and the conducting heat to the soil below. Generally, the distinct thermal environment of urban area's as a whole in the effects of heating process of traditional sealed surface and features of that are inherent in the built-up environment. Heating processes at the ground surface depend on radiative and heating properties of the ground surface materials such as

1 Department of Environmental Engineering & Pollution Control Shahjalal University Science & Technology Sylhet.

2 Department of Civil and Environmental Engineering, Saitama University, 255, Shemo - Okubo, Urawashi, Japan 338.

surface emission, reflectivity, thermal conductivity and also evaporation process at the surface.

Analysis of the response of the surface to atmospheric conditions is complicated due to non-linearities of the governing equations, the heterogeneity of the underlying soil and hysteresis of the moisture retention (Asaeda et. al., 1992). In this paper our effort has been focused to characterize the thermal behavior of alternate pavement materials other than traditional sealed materials in urban area which is known as porous pavement. To properly describe the interaction between porous pavement and urban atmospheric boundary layer, one must adequately describe heat and moisture movement at porous surfaces and within the soil below, since the soil layer represents both a source and a sink of heat and moisture to and from the atmosphere (Michael et. al. 1994). Two major impacts of urban surfaces on thermal environment are summarized as 'Heating process of a paved surfaces and anthropogenic heat release from domestic use, transportation and industry those are considered to be the most distinguished factor controlling the urban temperature excess over that of rural environment. In this study we gave emphasized on the investigation of heating processes inside the various paved surfaces based on the observational data and by means of a numerical model. In an effort to simulate these complicated characteristics a unidimensional model for the heat flow characteristics under the various covered surfaces has been employed.

MATERIALS AND METHODS

Heating Process of Pavement

Studies has (Eusuf et al., 1997) revealed that the main reason for the modification of urban thermal environment is the depreciation of the fraction of natural surface and expand the impermeable paved surfaces in the urban area. Pavement other than impermeable has followed the similar mechanism of radiation transport, in which a large part of net downward infrared radiation is converted into latent heat due to phase changes which is analogous with energy budget activities with usual natural surfaces covered by bare soil or vegetation. This makes temperature of the non-impermeable paved surfaces not to escalate much, and subsequently the underground heat storage and sensible heat exchange between the ground surface and atmosphere are diminutive. For such a ground surface, the heating of the atmosphere by sensible heat released from the ground surface is present only during the day. After sunset, temperatures of the that ground surface other than impermeable decline quickly and soon become lower than that of the atmosphere. Hence at night, the downward transfer of the sensible heat from the atmosphere to the ground surface leads to the cooling of the atmosphere by the ground surface. However, this phenomenon is completely different for the case of a impermeable or nonporous pavement surface. During the

day, nonporous pavement surface absorbs a large amount of solar radiation (because of smaller surface reflectivity); and since no evaporation can occur, this makes nonporous pavement surface temperature significantly higher than that of the overlying atmosphere. This high surface temperature makes higher sensible heat exchange between the surface and the atmosphere and higher net upward long wave radiation from the surface, causing higher air temperature in the urban area compared with that in the rural area. Also the high conductivity of the nonporous pavement material help it store a large amount of heat during the day. This subsurface heat storage is released to the atmosphere at night in the form of sensible heat and upward long wave radiation. Hence the temperature of the atmosphere above an urban surface is higher than that above the rural surface not only during the day, but also at night, which causes the so called nocturnal urban heat island.

It is clear that of the above mentioned factors must be accounted for investigation of the thermal characteristics of porous pavement.

Observational Work and Data Collection

A series of observations were conducted throughout the year from August, 1994 to July, 1995 at the Housing & Urban Development Corporation office at Kuki, 70 km north of Tokyo (36°N, 139°36'). These observations were aimed at primarily to investigate the heating processes inside various pavements. There were ten types of sample paved surfaces prepared for the observation of surface temperature and temperature at various depths under the surface together with ground heat flux. Additionally surface reflectivity, atmospheric conditions such as air temperature, relative humidity and wind velocity, downward total solar radiation, infrared radiation were also measured. Although measurements were carried out throughout one year as it is the intended to study the effect of various pavements on near surface atmospheric environment during hot summer days, in this paper only results of observation in 9-10 August, 1994 are presented. Five adjoing sample surface materials out of ten with contrasting thermal properties which consisted to porous block pavement, brick, fresh dark non-porous asphalt, grass (3.0 cm long) and ceramic porous pavement were selected for this study. The physical characteristics of the samples have been presented in Table 1. Ambient atmospheric temperature, relative humidity and wind velocity were measured in a standard meteorological height 2.0 m above the sample surfaces. The measuring instruments were installed at this level to measure the meteorological conditions for the evaluation of energy balance of the concerned samples together with necessary parameters. Arrangement of measuring instruments is shown in Table 2.

Table 1. Physical Characteristics of different Pavements

Pavement Name	Description of Pavement
1. Porous 1(Sample A)	Block sizes are 30X30 cm. Thickness is 6 cm. Subsurface temperature observed at 3, 6, 24 and 54 cm from surface.
2. Brick (Sample C)	Clay burnt Brick Block. Size is 20X10X6cm. Subsurface temp. Observed at 3, 6, 24 and 54 cm from surface.
3. Asphalt (Sample E)	Thickness is 5cm Subsurface temperature observed at 2.5, 5, 25 and 55cm from surface.
4. Grass (Sample F)	Natural green grass, 1-3cm long and sub-surface temperature observed at 2.5 and 5cm from surface.
5. Ceramic (Sample H)	Thickness is 2.5cm. Block size is 10X10X2.5cm Subsurface temperature observed at 1.25, 2.5, 28.5 and 58.5cm from surface.

Table 2. Arrangement of measuring instruments

For all Sample	Measuring Instrument	Accuracy	Measurement Intervals
1 Air Temp Relative humidity	Platinum-wire thermometer electostatical capacitance type	VAISALA IMP 130Y ±0.2°C, ± 2%	10 minute
2 Surface and Sub surface. Temperature	CCTT	± 0.2oC	10 minute
3 Wind velocity	3-cup anemo-meter	-0.3m/s	10 minute
4 Albedo	Albedometer	Eko ER-91-02015	15minute
5 Heat flux conducted into ground	Heat flow-meter	Eko MF-81	10 minute
6 Surface infrared radiation	Radiation thermometer	Eko MF-1010	10 minute

Fig. 1 depicts relative humidity, wind velocity and air temperature recorded at the observational site on August 8-9, 1994. As in the fig., during the day, air temperature reached approximately about 35°C at noon, while the wind velocity was about 4m/s and relative humidity was about 43%. These conditions are believed to be that of typical summer days in that area (Kuki).

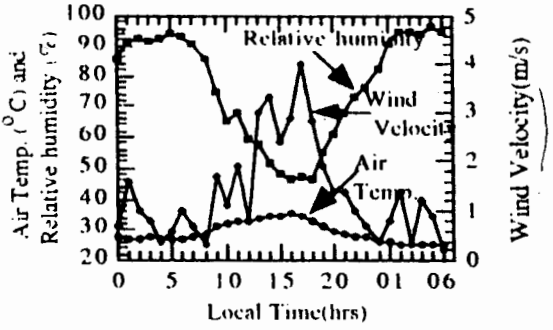

Fig 1. Meteorological conditions at 9-10 August, 1994.

During the observation surface reflectivity or albedo was measured using the instrument as presented in Table 2. The recorded data were in two parts such as incoming solar radiation incident on the surface and part of that reflected by the surface to the atmosphere. This is used for computing the surface reflectivity or albedo which is very important for the identification of radiative characteristics of concerned incidental surface and the values completely depend on the solar local altitude or solar zenith angle as well as day of the year, angle of solar declination, latitude of the place and solar hour angle. The observed values of reflectivity for different surfaces are presented in Table 3.

Table 3. Radiative Properties of Pavement

Pavement	Reflectivity (at noon)	Surface Thermal Emissivity (es)
1. Porous 1	0.27	0.94
2. Brick	0.26	0.92
3. Asphalt	0.08	0.97
4. Grass	0.20	0.98
5. Ceramic	0.43	0.98

The surface temperatures were obtained by two way; the emitted infrared radiation from the surface and from the sample skin temperature which was measured by the copper constantan and thermocouple (Table 2). Infrared radiation from the surface was observed

using the instrument of hand held type radiation thermometer (Table 2) and data were evaluated for the surface temperature by using the relation of Stefann Boltzmann constant and surface emissivity. This evaluated surface temperature is known as brightness or apparent or radiative temparature.

The target was chosen as near as possible to be the representative sample surface conditions and equal weight was given to the all sample surfaces. The studied surfaces and data were measured through the data logger & recorder (Model Chin). A significant variation was found between radiative surface temperature and the temperature measured by the thermocouple, it was due the influence of surface emissivity (Griend et al., 1991). The surface emissivity was evaluated by using the measured pavement surface temperature directly by thermal sensor and the upward infrared radiation and estimated value for the emissivity of various sample surface has presented in Table 3.

Sub-surface temperature under the porous and nonporous pavement was obtained using thermocouple at different depths, the measurement levels of subsurface temperature are depicted in Fig. 2. For the

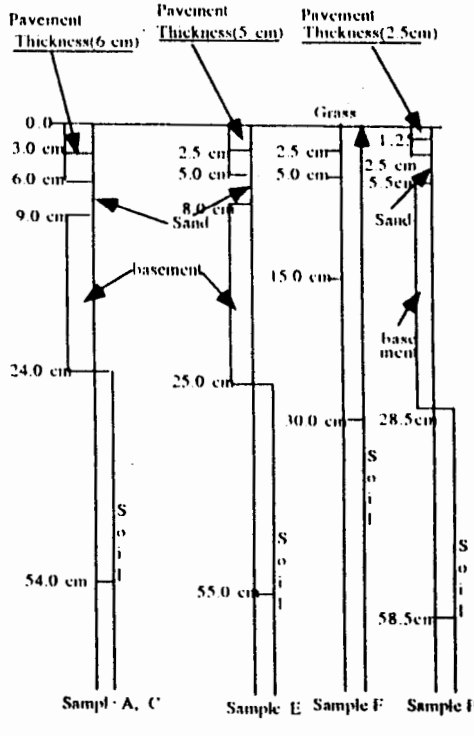

Fig 2. Subsurface Profiles Distribution.

measurement of ground heat flux, heat flow meter was installed at the interface of sand and basement packing below the sample surfaces. Hydraulic characteristics such as porosity, hydraulic conductivity, percentage of water content, dry density of each sample pavement materials were estimated through the experiment in the laboratory. The thermal properties such as specific heat, thermal conductivity and heat capacity for each sample materials were estimated also through the laboratory experiment. The experimental results which have been used in the model as input parameters are given in Table 4 and Table 5.

Table 4. Hydraulic Properties of Pavement Materials

Pavement	Porosity	Dry Density (Kg/m^3) ($X10^3$)	Water content (%)	Wet Density (Kg/m3) ($X10^3$)
1. Porous 1	0.30	1.913	15.60	2.211
2. Brick	0.32	1.903	11.30	2.209
3. Ceramic	0.44	1.442	28.40	1.851

Table 5. Thermal Properties of Pavement Materials

Pavement	Density P_s (Kg/m^3)	Sp. heat ($J.Kg^{-1}K^{-1}$) $X10^2$	Thermal Conduct ($J.s^{-1}m^{-1}K^{-1}$)	P_c ($J.m^{-3}K^{-1}$) $X10^6$
1. Porous 1	2347	7.25	1.228	1.70
2. Brick	1850	7.548	0.829	1.40
3. Asphalt	2110	9.253	0.811	1.95
4. Grass 1	600	8.0	0.28	1.28
5. Ceramic	1526	9.08	1.199	1.37

Numerical Computation

The present model attempts to estimate the thermal behavior of surface materials. In order to solve this problem, a mathematical model is employed to simulate the thermal phenomena of surface covered by porous, grass and non-porous materials. The governing equations for mass and heat transfer under the sample surfaces are as follows. The eq. of mass transfer inside the porous pavement is as Eq.(1)

$$\left[\left(1-\frac{p_v}{p_e}\right)\frac{\partial\theta}{\partial\psi}+\frac{\theta_a\,\partial p_v}{p_e\,\partial\psi}\right]\frac{\partial\psi}{\partial t}+\left[\left(1-\frac{p_u}{p_e}\right)\frac{\partial\theta}{\partial T}+\frac{\theta_a\,\partial p_v}{p_e\,\partial T}\right]\frac{\partial T}{\partial t} \qquad (1)$$

$$= \Delta[(K+D_{\psi\upsilon})\,\Delta\Psi+(DT\upsilon+DTa)\,\Delta T]+\frac{\partial k}{\partial z}$$

The corresponding eq. for heat transfer is

$$\left[C+L\theta_a\frac{\partial \rho_\upsilon}{\partial T}(P_eW+\rho_\upsilon L)\frac{\partial \theta}{\partial T}\right]\frac{\partial T}{\partial t}+\left[L\theta_a\frac{\partial P\upsilon}{\partial \psi}(P_eW+P_\upsilon L)\frac{\partial \theta}{\partial \psi}\right]\frac{\partial \theta}{\partial t} \qquad (2)$$

$$= \Delta[\lambda\Delta T+P_e(LD\,\Psi\upsilon+gTD_{Ta})\,\Delta\Psi]-C_e\,qm\,\Delta T$$

Where C is the total volumetric heat capacity of the soil and is estimated by

$$C=C_d+C_e\rho_e\theta+C_p\rho\upsilon\theta_a$$

The vapor density is given by

$$\rho\upsilon(\psi,T) = \rho_u(T)\exp(\psi g/RT_k) \qquad (3)$$

Where θ is the volumetric liquid water content, θ_a is the volumetric air content, t is the time, z is the depth Cp is the heat capacity of dry soil, is the specific heat of vapor at constant pressure,W is the differential heat of wetting. ρ_o is the saturation vapor density at temperature T, R is the gas constant for water vapor, T_k is the absolute temperature, q_m is the moisture flux, P_e is the liquid water density, $D\psi\upsilon$ is the matric potential diffusivity of water vapor, $DT\upsilon$ is the temperature diffusivity of vapor and DTa is the transport coefficient for absorbed liquid flow due to thermal gradient, T is the temperature, ψ is the matric potential, K is the hydraulic conductivity and κ is the unit vector opposite of gravity. C_e is the heat capacity of liquid water, L is the latent heat of vaporization. The evaluation of other coefficients of Eq. (1) and Eq. (2) are described by (Asaeda, T. et. al., 1992).

The heat conservation eq. for non-porous pavement is (Eusof at el)

$$\rho c\frac{\partial T}{\partial t}=K_1\frac{\partial^2 T}{\partial z_2} \qquad (4)$$

Where ρc, K_1 are heat capacity and thermal conductivity of surface covering materials respectively. The equations of mass and heat conservation inside the soil below the pavement materials are the same as Eq.(1) and Eq.(2).

The top surface boundary conditions are the mass and heat fluxes at the surface. The surface mass flux is the rate of evaporation (Milly et al., 1976)

$$qm=e \qquad (5)$$

The surface boundary condition for heat flux is as follows:

$$-K_1 \frac{\partial T}{\partial z} = R_{net}+H-Le-C_e(T-T_o)e \quad (6)$$

Where the first term of the right hand side R_{net} is the net radiation flux, the second term *H* is the turbulent sensible heat flux and the third term is the turbulent latent heat flux, T_o is the reference temperature as the datum of or zero enthalpy (Asaed et al., 1992; Philip et al., 1957. The fourth term is the sensible heat carried from the porous surfaces to the atmosphere by the evaporated water vapor. For non-porous materials such as asphalt, the third and fourth term of Eq. (6) is absent since no evaporation can occur at these surfaces and e is the rate of evaporation.

The net radiation flux density R_{net} is estimated from (Aseda et. al.1992, Hoffest et. al 1979 and Novak et. al. 1985)

$$R_{net} = (S_o/r^2)(0.6+0.2sinZ)cosZ(0.05+0.1(1-cosZ))(1-0.65n) \quad (7)$$

$$(1-\alpha)+\varepsilon_s[\varepsilon_a T_a^4(d,t))-(T_s^4 s(o, t)]$$

In Eq.(7) there are two parts in right hand side, where first part for the determination of net solar irradiance flux on the surfaces including diffused and reflected solar radiation and atmospheric transmissivity and second part for the determination of net infrared radiation flux from the surfaces. Solar irradiance flux varies with the altitude angle or solar zenith angle Z which is the function of latitude of the location, declination and hour angle of the sun.

The effective emissivity from the atmosphere ε_a is the function of fraction of clear sky, the clear sky atmospheric emissivity and difference of cloud base-screen height temperature which has described in (Novak et al., 1985). $T_a(d,t)$ and $T_s(o,t)$ in Eq.(7) are the absolute temperature of the air and ground temperature respectively. Surface temperature has been considered from observation data.

It is generally assumed that a very simple representation of the drag at the surface is sufficient to account for the effect of the boundary layer fluxes and it is necessary to simulate the momentum and heat fluxes at the boundary. In order to include the effects of air stability, the drag coefficient in model has been modified by introducing the parameterization suggested by Louis (Louis, 1979). The atmospheric transport mechanism of water vapor is quite similar with that of the sensible heat (Asacda et al., 1992 and Louis, 1979). Hence, it is assumed that the evaporation rate e can be described in the same form of Louis description or sensible heat flux.

$$e = \rho_a(k^2/M)[ln(z/z_o)]^2 U_a \Delta \rho f e(z/z_o, R_i) \quad (8)$$

In Eq. (8) K is the Von Karman constant for stability, R_i is the bulk Richardson number of the layer, U_a is the wind velocity at reference state, $\Delta\rho$ is the difference of vapor density of the surface and the air, ρ_a is the density of air, z is the reference height (screen height) and z_o is the roughness of coefficient and M is the constant. The value of *M* and K are as 0.74 and 0.35 respectively.

The turbulent sensible heat flux, second term of right hand side of Eq. (6) can be determined by the following eq..

$$H = \rho_a C_d u^* \Theta^* \qquad (9)$$

$$= \rho C_a a[k^2/M][\ln(z/zo)]^{-2}\, Ua\Delta\, \Theta f_h(z/z_o, R_i)$$

The relation between the stability function f_h (in the case of sensible heat flux) of Eq.(9) and f_e (in the case of latent heat flux) of Eq.(8) can be determined from the best fit of observed surface temperatures and that of calibrated by the model. Let the determinant coefficient between f_h and f_e is c_1 and is expressed as, $f_e = C_1 f_h$.

The stability function f_h and f_e are the function of ratio of reference height to the surface roughness and Richardson number R_i, if $R_i \geq O$ shows the stability and $R_i \leq O$ in case of instability. The form of these stability functions have been given else where in (Aseda et al., 1992 and Louis 1979). The lower boundary condition is at large depth, temperature is constant and equals to 27.5°C and depth considered for simulation is 2m from the surface of the materials. The initial value for *T(z)* was specified from the observational data. The initial conditions are given temperature and matric head at time $t=t_o$ at the beginning of the computation time.

RESULTS AND DISCUSSIONS

Temperature Distribution of the Surface and Subsurface of the Sample

The energy budget of the near surface atmosphere depends on the pavement surface temperature which turns into the thermal processes below the surface Fig. 3(a-d) depict the vertical profile of surface and subsurface temperatures of samples (Table 1) in various layers as on Fig. 2 and using the instruments which are described in Table 2 at different meteorological diurnal transition period 6:00, 12:00, 18:00 and 0:00 in August 9-10, 1994 at Kuki. These distinct times were adopted since the multiform of thermal characteristics can be found in this period. In the mentioned transition period; one is just after sunrise, an isothermal condition in nature; the other is at noon, warmer than the normal or

desirable; another is the late afternoon before sunset, diverse to cooling process time in a day; and the last one is in the mid night, a stable condition of the day.

Figure 3(a) depicts the temperature distributions in all samples at 6:00 just after sunrise. Temperature of all surfaces remained low but the subsurface thermal gradients were negative and toward the surface, due to the fact that heat stored during the following day was being released. On the other hand, in spite of the differences in the pavement materials, the surface temperature distribution is in close proximity. Subsurface temperature about 20cm below the surface was found maximum due to the fact that energy storage is higher up to that depth. Temperature at 20cm under the surface covered by the nonporous asphalt or porous block are nearly same, which is about 6°C, 4°C and 2°C higher than that of under surface covered by natural grass, brick and ceramic respectively. Under the surfaces, temperature decreases from large depth towards the surfaces, which indicates that the stored heat was released. Fig. 3(b) depicts the vertical profile of temperature distribution at noon, when all sample surface temperatures are higher than the sub surface, because in this transition period all surfaces absorb solar energy according to their surface reflectivity (Table 3) and stored heat energy to the subsurface. A large diversification in the thermic rate can be seen among the pavement substance. The surface temperature of asphalt is higher than that of the other pervious paved surfaces or natural grass. The subsurface temperature differences of asphalt and porous block are nearly the same at about 20cm depth from the surface, which is also about 6°C higher than that under surface covered by brick, ceramic or natural grass surface. The temperature under 20 cm below of the asphalt pavement is lower than the porous block and decreases more rapidly. This is due to the fact that heat conductivity of porous block is higher than the asphalt and also due to the effect of water content and the net heat flux at the surface of nonporous pavement is used for heating the surface layer of pavement. Thus it can be expected that the storage below the porous block is larger than the nonporous pavement during the thermal period from morning till afternoon. Fig 3(c) is data at 18:00 just before the sunset and Fig. 3(d) is data at 0:00. From the Figs 3(a-d) it is found that the subsurface temperature under the ceramic surface is lower than that of porous block or asphalt and is higher than natural grass and brick. It is due to the effect of moisture content which significantly changes the heat capacity. conductivity and diffusivity of subsurface materials. The temperature of

the natural grass surface is less than that of other surfaces due to evapotranspiration from grass surface and the distribution of temperature under the grass is very different from that under other surfaces. The diurnal surface temperature of asphalt and porous block decreases to less than 32°C and grass surface temperature decreases to less than air temperature. Vertical temperatures difference at depth 20 cm was observed about 6°C at 18:00, 4.5°C at 0:00. Compared with Figs. 3(b), 3(c) and 3(d) we can see that temperature difference between the three figures is the amount of heat released to the atmosphere. Among the pavement temperature it is observed that the surface temperature of porous block is higher because of pore size; its bulky pore size reduces the capillary pressure, sequentially impede the evaporation from the surface and surface is heated, on the other hand ceramic pavement absorb large amount of water from the underlying soil layers by capillary pressue through minuscute type of pore, which is in turn to the evapoated and released to the atmosphere. Surface heat input was conducted downward more rapidly compared to the porous pavement and the natural grass surface, storing a significant amount of heat inside the pavement during the day, which was then released at night. To make it easier for comparison of temperature distribution at surface and subsurface of various samples with different thickness in different times are show in Fig. 4(a-e). Temperature at the nonporous asphalt pavement at the peak hour was more than 52°C, which was 17°C higher than air temperature (Fig. 1) and temperature of the other sample surfaces such as porous block, brick. ceramic and natural grass reached about 48.5°C, 42.4°C, 42.7°C and 43°C respectively. The data of air is standard data of mid-latitude in summer. However, temperature at the ceramic pavement is much lower than that of other surfaces and almost the same as natural grass or brick pavement at noon. At nonporous pavement after reaching the maximum value at 13:00, the surface temperature decreased, due to heat exchange with cooler overlying atmosphere and conducted downwards to deeper layers of the soil. This image was successfully reproduced using the numerical model coupling subsurface heat and moisture transfer. Results of the computations revealed that pore volumes inside the porous pavement is very important for the transport of water vapor. Large pores reduce the capillary pressure, trapped the evaporation from the surface. The comparison of simulated and observed temperature distributions for different sample surfaces with various depth at different times in a day is already presented in Fig. 3 and in Fig.

4. The figures are evident that there is a good agreement between observed and simulated data.

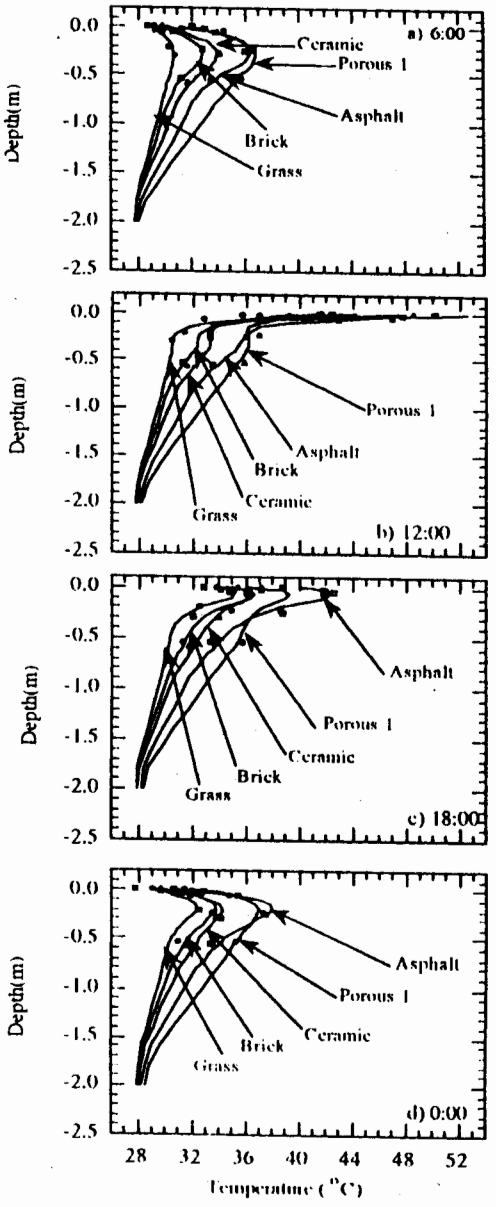

Fig 3. Vertical Profiles of Temperature Distribution. Symbol for Observed Data and Line for Calculated a) 6:00, b) 12:00, c) 18:00 and d) 0:00.

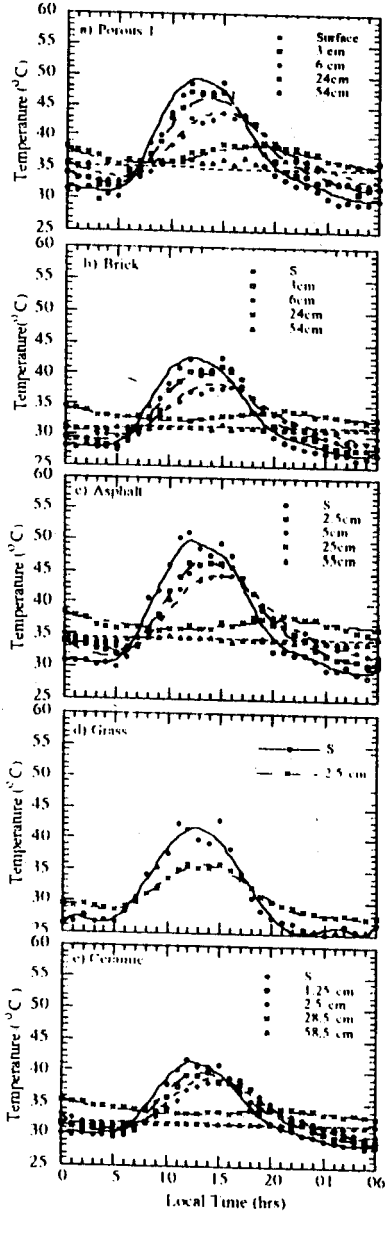

Fig 4. Diurnal Temperature Distribution at Various Depth of Samples. a) Porous 1, b) Brick, c) Asphalt, d) Grass and e) Ceramic.

Heat and Energy Fluxes at the Pavement Surface

Figures 5(a-e) show the component of the energy budget at the sample surfaces in August 9-10, 1994. In the fig. net radiation component was calculated using the Eq. (7). The turbulent transport of sensible and evaporation rate were calculated using the Eq. (8) to (9). The determinant coefficient C_1 is depended on the sample surfaces physical characteristics. It is reported as 0.44 for porous block, 0.58 for brick, 0.61 for ceramic and 0.73 for natural grass. Sign convention of the Fig. 5 upward is positive in case of net radiation, latent and conduction heat flux and downward is positive in the case of sensible heat flux. Inspection of Figs. 5(a-e) reveal that H for the nonporous asphalt pavement was almost the largest during the diurnal period, clearly owing to the large R_{net} value as well as available energy (R_{net} -G), whereas the smallest H value throughout the day was found for the natural grass. The smallest sensible heat for the natural grass surface was clearly a result of advection caused by its lower surface temperature. Also noticeable factors in these figures are that H on the asphalt surface remain positive even in the night time and gives largest value mainly because of the high surface temperature. Diurnal variations of L_e are shown also in Fig. 5, it can be seen that the largest portion of net radiation of the natural grass surface is converted to latent heat, L_e. At noon, with the net radiation reaching the grass surface of 587 W/m2, the latent heat flux is 475W/m2 while the sensible heat is only 92 W/m2 and heat flux to the ground 141 W/m^2. L_e for porous1 is smaller than natural grass or other surfaces. It is due the evapotranspiration through grass surface and volume of pore size in porous 1. Pore volume inside the porous pavement has played a significant role for transfer of water vapor which as already been discussed. For the asphalt pavement, since there is no evaporation from its surface, in the total 630 W/m^2 of net radiation to its surface, 410 W/m^2 becomes sensible heat and 200 M/m^2 becomes the heat flux G to the ground. The sensible heat flux from the asphalt pavement directly heats the atmosphere while the conduction heat to the ground is released at night to the atmosphere, causing the nocturnal heat island. Also it can be noticed that peak hour of L_e for different sample surfaces are significantly different although the peak hour of R_{net} for all the sample surfaces are nearly the same.

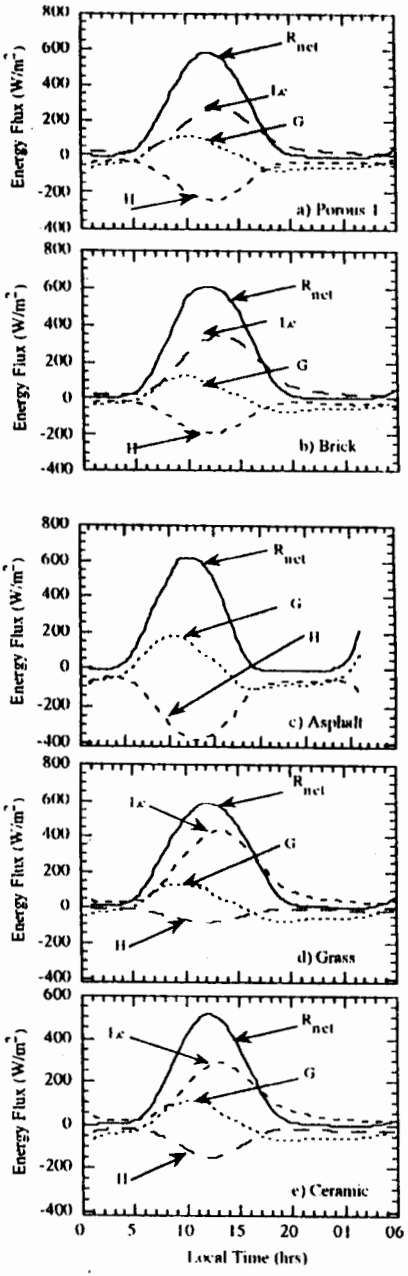

Fig 5. Energy Budget at the Sample Surfaces. a) Porous 1, b) Brick, c) Asphalt, d) Grass and c) c)Ceramic.

Hysteresis effect at the Porous Pavement

Hystersis of surface moisture retention characteristics was measured by the laboratory experiment using tensiometer. It was found that in case of sample H, when it is dried continuously from saturated condition the matric potential decreases monotonically from zero to some value near ψ =103.3 (pE=3.3) and θ = 7.36. The drainage and wetting curves form a closed loop, which is depicted in the Fig. 6 for the sample Ceramic. As drainage progress, it was found that a certain quantity of water remains (in the form of immobile thin film) in the sample even at very high capillary pressures, this value in Fig. 6 is denoted by θ_0. θ_0 also known as irreducible water content. pF is a term of oftenly used to showing the pressure or matric head value in wide range in a single diagram, it is defined as pE=log(- ψ).

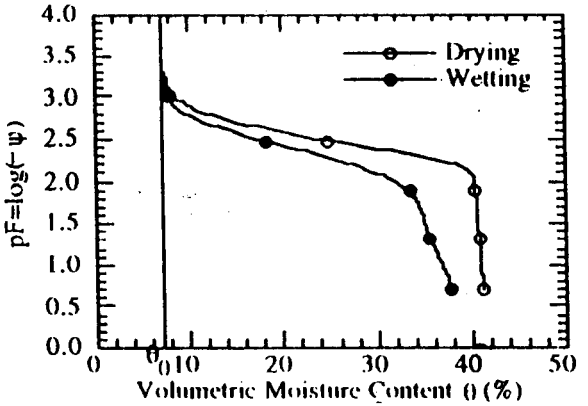

Fig 6. Hysteresis Effect in Surface Moisture Retention of the Ceramic Sample H.

CONCLUDING REMARKS

A study of the thermal transfer to the underground of the porous pavement can not be handled properly without the coupling of moisture and heat transfer. Because of evaporation from porous surface and evapotranspiration from grass surface, the temperature of the porous pavement surface is smaller than non-porous surface. The nonporous surface materials can absorb a large amount of the incoming net radiation, which increases its surface temperature and causes the variation of urban thermal environment. The evaporation and condensation of water inside the subsurface of pavement regulate the surface temperature, so increase the pavement thickness of nonporous pavement makes urban thermal environment more serious. From the observation of kuki 94, it is evident that porous pavement is more reliable than that of the nonporous pavement for balancing the urban

themal environment. Our next attempt is to investigate the effect of porous pavement on the heating of urban canopy and make an effort to predict a comfortable summer thermal equality.

REFERENCES

Asaeda T. and Ca V.T. (1992), 'The Subsurface Transport of Heat and Moisture and Its Effects on Environment : A Numerical Model. Boundary Layer Meteorology15-16, 253-261.

Michael Ek and Cuenca R.H, (1994), 'Variation in Soil Parameters Implications For Modeling Surface Fluxes and Atmospheric Boundary-layer Development', Boundary Layer Meteorology, Vol. 70, 369-383.

Dullien F.A.L. (1991), Characterization of Porous Media', Transport in Porous media Vol. 6, 581-606.

Eusuf M.A. Asaeda T. and Ca V.T 'A Parameterization of Convective heat exchange between urban canyon and atmosphere', (Submitted to the Journal of Energy and Building)

Eusuf M.A., Ca V.T, Asaeda T. and Ozaki. (1995), "Thermal Characteristics of porous Pavement and its Effect on Urban Environment". Environmental System Research, Japan, Vol. 23,

Milly P.C.D, (1976), 'A Simulation Analysis of Thermal Effects on Evaporation from Soil, Water Resources Research, Vol. 12, No.6, 1284-1254.

Philip J.R and De Vries D.A, (1957), 'Moisture Movement in Porous Materials under Temperature Gradient', Transactions, American Geophysical Union, Vol. 38, No. 2, 222-232.

Louis J.F, (1979), 'A Parametric Model of Vertical Eddy Fluxes in the Atmosphere', Boundary Layer Meteorology', 17, 429-442.

De Griend A.A.V. Owe M., Grom M. and Stoll M.P. (1991) 'Measurement and Spatial Variation of Thermal Infrared Emissivity in Savanna Environment', Water Resources Research, Vol. 27, No.3, 371-379.

Hoffert M.I and Storch J., (1979), 'A Scheme For Computing Surface Fluxes from Mean flow Observations', 'Boundary Layer Meteorology', 17, 429-442.

Novak M.D. and Black T.A, (1985), 'Theoretical Determination of the Surface Energy Balance and Thermal Regimes of Bare Soils', Boundary Layer Meteorology', 33, 313-333.